



Synthesis of salen Mn(III) immobilized onto the ZnPS-PVPA modified by 1,2,3-triazole and their application for asymmetric epoxidation of olefins



Jing Huang^{a,*}, Jiali Cai^b, Hao Feng^a, Zhiguo Liu^a, Xiangkai Fu^c, Qiang Miao^c

^a School of Physics and Chemistry, Xihua University, Chengdu, 610039, PR China

^b College of Rongchang Southwest University, Chongqing 402460, PR China

^c College of Chemistry and Chemical Engineering Southwest University, Research Institute of Applied Chemistry Southwest University, The Key Laboratory of Applied Chemistry of Chongqing Municipality, The Key Laboratory of Eco-environments in Three Gorges Reservoir Region Ministry of Education, Chongqing 400715, PR China

ARTICLE INFO

Article history:

Received 6 December 2012

Received in revised form 18 April 2013

Accepted 23 April 2013

Available online 28 April 2013

Keywords:

Chiral Mn(III) salen

Zinc poly(styrene-phenylvinylphosphonate)-phosphate

Heterogeneous catalyst

Asymmetric epoxidation

Click chemistry

ABSTRACT

A series of chiral salen Mn(III) complexes immobilized onto ZnPS-PVPA modified by 1,2,3-triazole through click chemistry were synthesized. High yields and comparable enantioselectivities were achieved in asymmetric epoxidation of unfunctional olefins with NaClO/PPNO and *m*-CPBA/NMO as well as NaIO₄/imidazole as the oxidative systems. The catalytic results indicated that the catalysts were selective for oxidative systems and the additives played different roles in different oxidative systems. Moreover, the superior reusability and catalytic abilities in large-scale reactions at the same level demonstrated the potentiality for application in industry.

© 2013 Elsevier Ltd. All rights reserved.

1. Introduction

The discovery of efficient and atom-economic catalyst systems for asymmetric epoxidation is an important objective of catalytic chemistry.¹ The dominant catalytic approaches toward obtaining enantiomerically pure compounds are homogeneous catalysis, which includes transition metal catalysis,² organocatalysis,³ and bio-catalysis.⁴ Until recently, these approaches to catalysis have developed in parallel as separate fields. Over the last decade, however, significant efforts have been made to bridge the gap between these fields.⁵

The Huisgen 1,3-dipolar cycloaddition reaction broadly known as click chemistry of organic azides and alkynes^{6,7} has gained considerable attention in recent years, which is an efficient way to produce 1,4-disubstituted 1,2,3-triazoles. Click chemistry is not a scientific discipline but rather a synthetic philosophy inspired by the simplicity and efficiency of the chemistry that takes place in nature. Moreover, the objective of click chemistry would be to

establish an ideal set of straightforward and highly selective reactions in synthetic chemistry.^{8–14}

Although click chemistry was initially postulated as a general concept for organic synthesis, this strategy was seldom introduced into the synthesis of the catalyst and even less applied in the immobilization of chiral salen Mn(III). In addition, many efforts have been made to develop recyclable catalysts by supporting catalytically active chiral metal complexes onto organic or inorganic supports^{15,16} and ionic liquids.^{17,18} Herein, we wish to report a new, simple bifunctional, recoverable, and reusable heterogeneous chiral salen Mn(III) catalyst that promotes asymmetric epoxidation reactions while achieving a respectable level of enantioselectivity, and this catalyst can be used in large-scale reactions with the catalytic ability being maintained at the same level.

2. Experiment

2.1. Materials and instruments

(1*R*,2*R*)-(–)-1,2-Diaminocyclohexane, chloromethyl methyl ether (toxic compound), α -methylstyrene, *n*-nonane, *N*-methylmorpholine *N*-oxide (NMO), and *m*-chloroperbenzoic acid (*m*-CPBA) were

* Corresponding author. Tel.: +86 2887720037; fax: +86 2887720200; e-mail address: hj41012@163.com (J. Huang).

supplied by Alfa Aesar. Other commercially available chemicals were laboratory-grade reagents from local suppliers. Chiral salen ligand and chiral homogeneous catalyst salen Mn(III) were synthesized according to the standard literature procedures,¹⁹ and further identified by analysis and comparison of IR spectra with literature.²⁰

FT-IR spectra were recorded from KBr pellets using a Bruker RFS100/S spectrophotometer (USA) and diffuse reflectance UV–vis spectra of the solid samples were recorded in the spectrophotometer with an integrating sphere using BaSO₄ as standard. ¹H NMR and ³¹P NMR were performed on AV-300 NMR instrument at ambient temperature at 300 and 121 MHz, respectively. All of the chemical shifts were reported downfield in parts per million relative to the hydrogen and phosphorus resonance of TMS and 85% H₃PO₄, respectively. Number- and weight-average molecular weights (M_n and M_w) and polydispersity (M_w/M_n) were estimated by Waters1515 gel permeation chromatograph (GPC; against polystyrene standards) using THF as an eluent (1.0 mL min⁻¹) at 35 °C. X-ray photoelectron spectrum was recorded on ESCALab250 instrument. The interlayer spacings were obtained on DX-1000 automated X-ray power diffractometer, using Cu K α radiation and internal silicon powder standard with all samples. The patterns were generally measured between 3.00° and 80.00° with a step size of 0.02° min⁻¹ and X-ray tube settings of 36 kV and 20 mA. C, H, and N elemental analysis was obtained from an EATM 1112 automatic elemental analyzer instrument (Thermo, USA). TG analyses were performed on an SBTQ600 thermal analyzer (USA) with the heating rate of 20 °C min⁻¹ from 25 to 1000 °C under flowing N₂ (100 mL min⁻¹). The Mn contents of the catalysts were determined by a TAS-986G (Pgeneral, China) atomic absorption spectroscopy. SEM were performed on KYKY-EM 3200 (KYKY, China) micrograph. TEM were obtained on a TECNAI10 (PHILIPS, Holland) apparatus. Nitrogen adsorption isotherms were measured at 77 K on a 3H-2000I (Huihaihong, China) volumetric adsorption analyzer with BET method. The racemic epoxides were prepared by epoxidation of the corresponding olefins by 3-chloroperbenzoic acid in CH₂Cl₂ and confirmed by NMR (Bruker AV-300), and the gas chromatography (GC) was calibrated with the samples of *n*-nonane, olefins, and corresponding racemic epoxides. The conversions (with *n*-nonane as internal standard) and the ee values were analyzed by gas chromatography (GC) with a Shimadzu GC2010 (Japan) instrument equipped using a chiral column (HP19091G-B213, 30 m×30 m×0.32 mm×0.25 μ m) and FID detector, injector 230 °C, detector 230 °C. Ultrapure nitrogen was used as the carrier (rate 34 mL min⁻¹) with carrier pressure 39.1 kPa and the injection pore temperature was set at 230 °C. The column temperature for indene, α -methylstyrene and styrene was programmed in the range of 80–180 °C.

2.2. Synthesis of the support (Scheme 1)

2.2.1. Synthesis of styrene-phenylvinylphosphonic acid copolymer (PS-PVPA). PS-PVPA was synthesized according to the literature.²¹

2.2.2. Synthesis of zinc poly(styrene-phenylvinylphosphonate)-phosphate (ZnPS-PVPA). PS-PVPA (1.0 g, 1 mmol), sodium dihydrogen phosphate (0.62 g, 4 mmol), zinc acetate (1.1 g, 5 mmol), and Et₃N (0.68 g, 6.7 mmol) were used for the synthesis of ZnPS-PVPA according to the literature.²²

2.2.3. Synthesis of chloromethyl-zinc poly(styrene-phenylvinylphosphonate)-phosphate (ZnCMPS-PVPA). Chloromethyl methyl ether (9.3 mL), anhydrous zinc chloride (3.32 g, 24.34 mmol), and ZnPS-PVPA (5.0 g, 3.4 mmol) were applied in the preparation of ZnCMPS-PVPA in compliance with the article.²²

2.2.4. Synthesis of triazole modified zinc poly(styrene-phenylvinylphosphonate)-phosphate (ZnTPS-PVPA). To a solution of

2 (0.5 mmol) was added equal equimolar of NaN₃ at room temperature. After the reaction mixture was refluxed at 50 °C for 10 h, the azide **3**, 3-bromoprop-1-yne (1.8 mL, 23 mmol), sodium ascorbate (0.2 equiv), and copper (II) sulfate pentahydrate (0.1 equiv) were added in THF/H₂O successively. 2 h later, strong aqua were added to the system and the brown solid **4** was obtained through filtration and washing. IR (KBr): $\nu_{\max}/\text{cm}^{-1}$ 3025, 2926 (CH), 2920, 2851 (triazole), 2342 (O=P–OH), 1651, 1543, 1511, 1492 (–C₆H₅), 1261 (P=O), 699 (C–Br) cm⁻¹. Found: C, 42.61; H, 3.18; N, 10.62%. Calcd for C₁₀₄H₁₀₅N₂₄O₁₁P₃Br₈Na₂Zn₃: C, 43.96; H, 3.70; N, 11.84%.

2.2.5. Synthesis of aminomethyl-triazole-zinc poly(styrene-phenylvinylphosphonate)-phosphate (ZnTAMPS-PVPA). Proper amount of diamines (such as a: 1,2-ethylenediamine, b: 1,3-propanediamine, c: 1,4-butanediamine, d: 1,6-hexylenediamine) were mixed with ZnTPS-PVPA (2.68 g), Na₂CO₃ (4.24 g, 0.04 mol), and THF (10 mL). After the mixture was kept at 66 °C for 10 h, the resinlike product was filtered, washed, and dried in vacuo. The products were abbreviated as **5a**, **5b**, **5c**, and **5d** in turn. Compound **5a**, Found: C, 52.15; H, 5.82; N, 19.46%. Calcd for C₁₂₀H₁₆₁N₄₀O₁₁P₃Na₂Zn₃: C, 53.91; H, 6.03; N, 20.97%. Compound **5b**, Found: C, 54.26; H, 6.04; N, 19.28%. Calcd for C₁₂₈H₁₇₇N₄₀O₁₁P₃Na₂Zn₃: C, 55.19; H, 6.36; N, 20.12%. Compound **5c**, Found: C, 55.26; H, 6.15; N, 19.06%. Calcd for C₁₃₆H₁₉₃N₄₀O₁₁P₃Na₂Zn₃: C, 56.37; H, 6.67; N, 19.34%. Compound **5d**, Found: C, 57.12; H, 7.08; N, 16.51%. Calcd for C₁₅₂H₂₂₅N₄₀O₁₁P₃Na₂Zn₃: C, 58.48; H, 7.21; N, 17.95%.

2.3. Synthesis of grafting chiral salen Mn(III) catalyst onto ZnTPS-PVPA (Scheme 2)

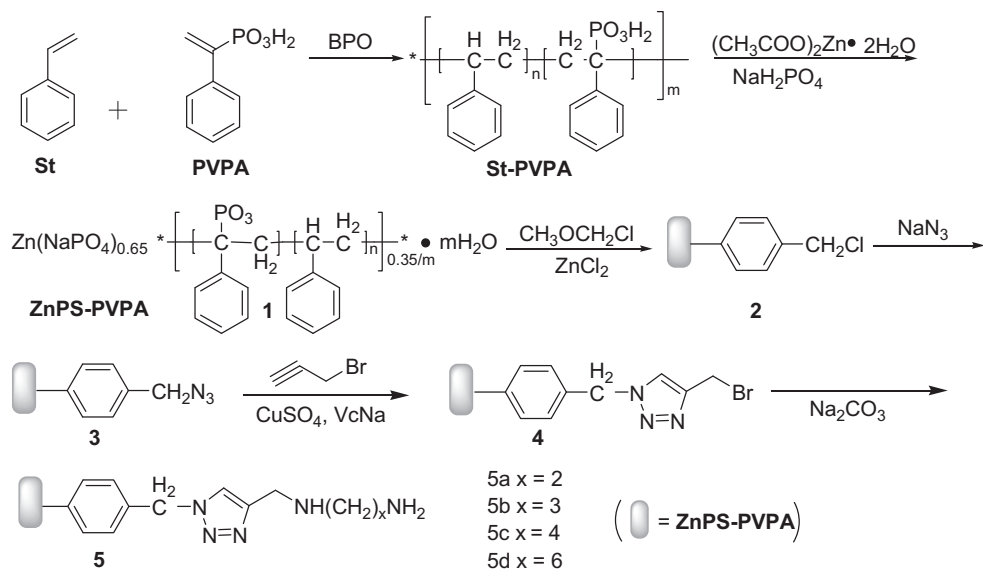
Chiral salen Mn(III) (4 mmol) in 10 mL of THF was added to the solution of **5** (0.5 g) and Et₃N (5 mmol). After the mixture was refluxed for 10 h, the solution was neutralized and the solvent was evaporated. The dark brown powder was obtained by filtration and washing. The products were abbreviated as **6a**, **6b**, **6c**, and **6d** in turn. Compound **6a**, Found: C, 64.12; H, 7.08; N, 9.54%. Calcd for C₄₀₈H₅₆₉N₅₆O₂₇P₃Na₂Zn₃Mn₈: C, 65.67; H, 7.63; N, 10.52%. Compound **6b**, Found: C, 64.15; H, 7.18; N, 9.24%. Calcd for C₄₁₆H₅₈₅N₅₆O₂₇P₃Na₂Zn₃Mn₈: C, 65.97; H, 7.73; N, 10.36%. Compound **6c**, Found: C, 65.27; H, 7.61; N, 9.85%. Calcd for C₄₂₄H₆₀₁N₅₆O₂₇P₃Na₂Zn₃Mn₈: C, 66.26; H, 7.83; N, 10.21%. Compound **6d**, Found: C, 65.27; H, 7.16; N, 9.23%. Calcd for C₄₄₀H₆₃₃N₅₆O₂₇P₃Na₂Zn₃Mn₈: C, 66.81; H, 8.01; N, 9.92%.

2.4. Synthesis of the homogeneous catalyst 10 (Scheme 3)

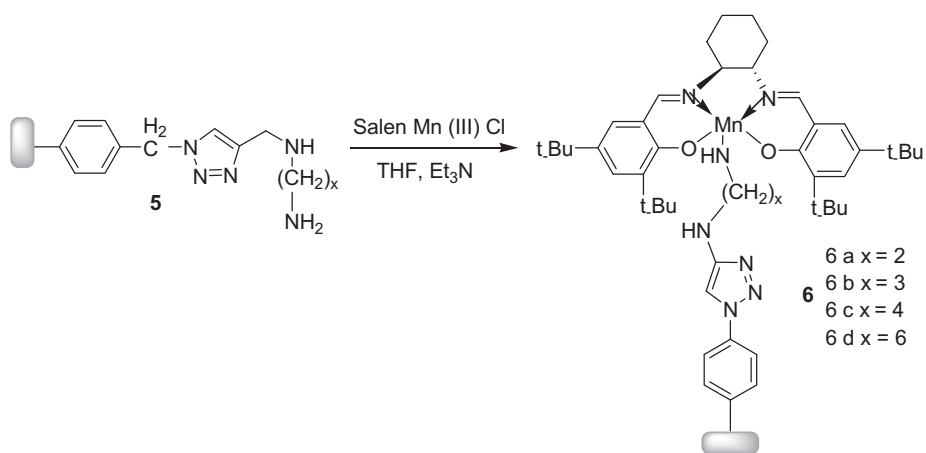
To a solution of benzyl bromide (4 mmol) was added equal equimolar of NaN₃ at room temperature. After refluxing at 60 °C for 10 h, the azide **7**, 3-bromoprop-1-yne (0.9 mL, 11.5 mmol), sodium ascorbate (0.2 equiv), and copper (II) sulfate pentahydrate (0.1 equiv) were added in acetone/H₂O successively. Then, 1,6-hexylenediamine (20 mmol), Na₂CO₃ (0.848 g, 8 mmol) were mixed with the compound **8** at 70 °C for 6 h to gain the compound **9**. The homogeneous catalyst **10** was synthesized according to the similar procedure to the supported catalyst **6d**. IR (KBr): $\nu_{\max}/\text{cm}^{-1}$ 3410, 1620 (–NH–), 3024, 2927 (CH), 2921, 2853 (triazole), 2339 (O=P–OH), 1651, 1543, 1513, 1492 (–C₆H₅), 1639 (–C=N) cm⁻¹, 1262 (P=O). Compound **10**, Found: C, 65.37; H, 8.12; N, 10.21%. Calcd for C₅₁H₇₄N₇O₂Mn: C, 66.81; H, 8.50; N, 11.25%.

2.5. Asymmetric epoxidation

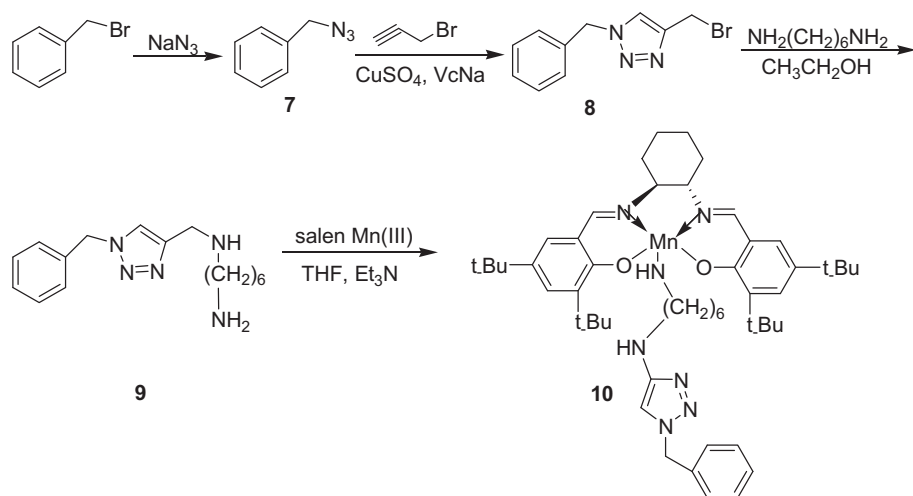
2.5.1. Using *m*-CPBA as oxidant. For *m*-CPBA/NMO system, the activities of the catalysts were tested for the epoxidation of unfunctionalized olefins in CH₂Cl₂ at –40 °C for 5 h with alkene (1 mmol),



Scheme 1. The synthesis of the supports.



Scheme 2. Synthetic route of the supported catalyst.



Scheme 3. Synthesis of the homogeneous catalyst 10.

n-nonane (internal standard, 1 mmol), NMO (5 mmol), homogeneous (5 mol %) or heterogeneous salen Mn(III) catalysts (5 mol %), and *m*-CPBA (2 mmol). After the reaction, Na₂CO₃ (2 mL, 1.0 M) was added to quench the reaction.

2.5.2. Using NaIO₄ as oxidant. For NaIO₄/imidazole system, the reactions were carried out in the 2:1 mixture of acetonitrile:water for 2.5 h at room temperature with alkene (1 mmol), NaIO₄ (2 mmol) in the presence of 5 mol % catalysts.

2.5.3. Using NaClO/PPNO as oxidant. For NaClO/PPNO system, to a solution of alkene (0.5 mmol), *n*-nonane (internal standard, 89.3 μL, 0.5 mmol), 4-PPNO (42 mg, 0.25 mmol), homogeneous (3 mol %) or heterogeneous salen Mn(III) catalysts (3 mol %), CH₂Cl₂ (4 mL), NaClO aqueous solution (pH 11.3, 0.55 M, 1.37 equiv, 1.25 mL) were added. The mixture was stirred at 25 °C.

2.6. The reusability of the catalyst

In a typical recirculation, the equal volume of hexane was added to the system after the reactions. Subsequently, the organic phase was separated. Then the catalyst was washed and dried over vacuum at 60 °C. In every run the same proportions of the substrate-to-catalyst and solvent-to-catalyst were retained.

2.7. General procedure for large-scale asymmetric epoxidation reaction

After the solution of catalyst **6d** (2.5 mmol), *n*-nonane (50 mmol), and α -methylstyrene (50 mmol) in CH₂Cl₂ (150 mL) at -40 °C was stirred for 30 min, *m*-CPBA (100 mmol) was added. Then, Na₂CO₃ (100 mL, 1.0 M) was added to quench the reaction. And the organic layer was dried over sodium sulfate. To follow, the catalyst was precipitated out from the solution by adding hexane. The conversions and ee values of the epoxide were determined by GC.

3. Results and discussion

3.1. Characterizations of the supports and the heterogeneous chiral catalysts

3.1.1. IR spectroscopy and UV–vis spectroscopy. The most informative evidence, which confirmed the anchoring of the chiral salen Mn(III)Cl to the triazole modified ZnPS-PVPA, was obtained by FT-IR spectra (Fig. 1). The band around 3408 cm⁻¹ was observed for the catalysts, which was assigned to the stretching vibration of

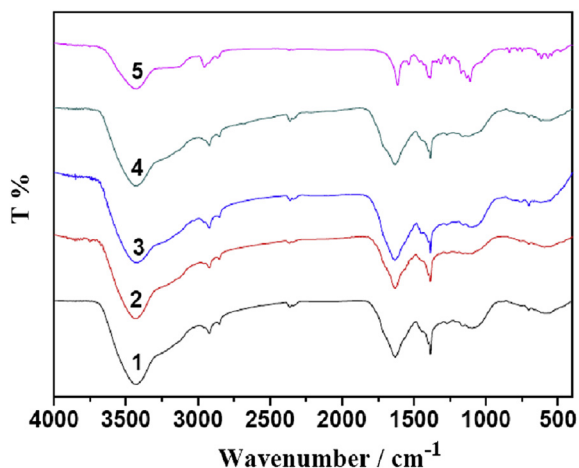


Fig. 1. FT-IR spectra of (1) **6a**; (2) **6b**; (3) **6c**; (4) **6d**; (5) the neat chiral salen Mn(III)Cl.

N–H groups. All the catalysts **6a–d** and chiral salen Mn(III)Cl had shown the same band at 1638 cm⁻¹, which was attributed to the vibration of imine group. The azomethene (C=N) stretching band of chiral salen Mn(III)Cl appeared at 1613 cm⁻¹ (5 in Fig. 1); while for the supported catalysts this band was also observed at the vicinity of 1617 cm⁻¹. The stretching vibration at 1030 cm⁻¹, which was assigned to characteristic vibrations of the phosphonic acid group in the support was obviously weakened due to the electronic structure changes for the host–guest interaction. In addition, the band at the hand of 1279 cm⁻¹ was put down to the vibration of triazole ring in the catalysts **6a–d**.

As described in Fig. S1, the spectras of catalyst **6a–d** have displayed similar features to those of chiral salen Mn(III)Cl on the basis of UV–vis observation. The bands at 335 nm could be attributed to the charge transfer transition of salen ligand. The band at 433 nm was due to the ligand-to-metal charge transfer transition, and the bands at 510 nm was assigned to the d–d transition of salen Mn(III) complex. There showed some deviations due to an interaction between the salen Mn(III) complex and the triazole modified ZnPS-PVPA.

3.1.2. Thermal gravimetric analysis. Shown in the TG curves (Fig. S2), with regard to **6d**, the initial weight loss was 2.2% below 180 °C. It was attributed to surface-bound or intercalated water in this stage. In the temperature range of 180–600 °C, the organic moieties decomposed with 33% weight loss. Obviously, catalyst **6d** still kept high stability lower than 180 °C. In general, organic reactions of heterogeneous catalysis were carried out below 180 °C. Therefore, the catalyst **6d** had adequate thermal stability to be applied in heterogeneous catalytic reactions.

3.1.3. Nitrogen adsorption–desorption isotherms. According to the catalyst **6d**, the nitrogen adsorption–desorption isotherms (Fig. 2) were characteristic type V, with a sharp increase in N₂ adsorption at higher P/P_0 values (~0.9) and a distinct hysteresis loop (type H₁). The pore diameters of the particles were mainly distributed between 2 nm and 15 nm, which was in the scope of mesoporous, and few particles were over 15 nm and less than 2 nm in diameter.

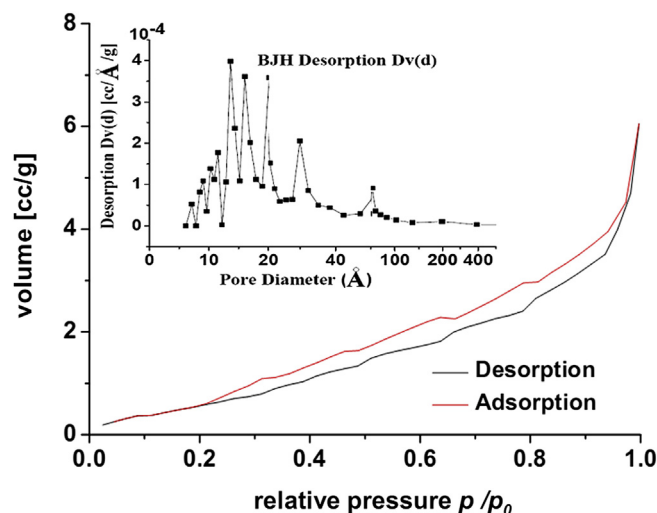


Fig. 2. The nitrogen adsorption–desorption isotherm and pore distribution of the catalyst **6d**.

The corresponding textural parameters calculated by N₂ adsorption–desorption isotherms were presented in Table 1.

Shown in Table 1, by means of chloromethylation, an obvious increase in BET surface area was observed (**1** vs **2**, from 4.9 to 36.9 m²/g) and increase in the pore volume (**1** vs **2**, from 1.3 to

Table 1
Physiochemical characterization data of **1**, **2**, and **6d**

Sample	Surface area (m ² /g)	Pore volume (×10 ⁻² cm ³ /g)	Average pore diameter (nm)
1	4.9	1.3	3.5
2	36.9	18.82	10.21
6d	5.16	1.05	5.94

18.82 × 10⁻² cm³/g) as well as in average pore diameter (**1** vs **2**, from 3.5 to 10.21 nm). It was due to that the chloromethylation of the support made the interlayer distance enlarged and the chloromethyl was relatively small so that BET surface area, pore volume, and pore diameter still increased. Compared with this phenomenon, a decrease in BET surface area (**2** vs **6d**, from 36.9 to 5.16 m²/g), in pore volume (**2** vs **6d**, from 18.82 to 1.05 × 10⁻² cm³/g), and in average pore diameter (**2** vs **6d**, from 10.21 to 5.94 nm) was observed upon immobilization of chiral salen Mn(III) onto ZnPS-PVPA modified by triazole. Although the interlayer distance augmented after the chloromethylation, some caves, holes as well as channels were occupied by salen Mn(III) owing to the steric bulky salen Mn(III) introduced in ZnPS-PVPA, further leading to the decrease in these structural parameters. In view of this facts, it could be deduced that few parts of chiral salen Mn(III) complexes were immobilized on the external surface of ZnPS-PVPA and major parts of chiral salen Mn(III) complexes were inserted into the mesopores.

3.1.4. Analysis of surface morphology. Shown in Fig. 3, SEM image of catalyst **6d** indicated that the amorphous structure was loose. And various caves, holes, porous as well as channels with different shape and size were existed in every particle. Some micropores and secondary channels would increase the surface area of the catalyst and provide enough chance for substrates to access to the catalytic active sites.

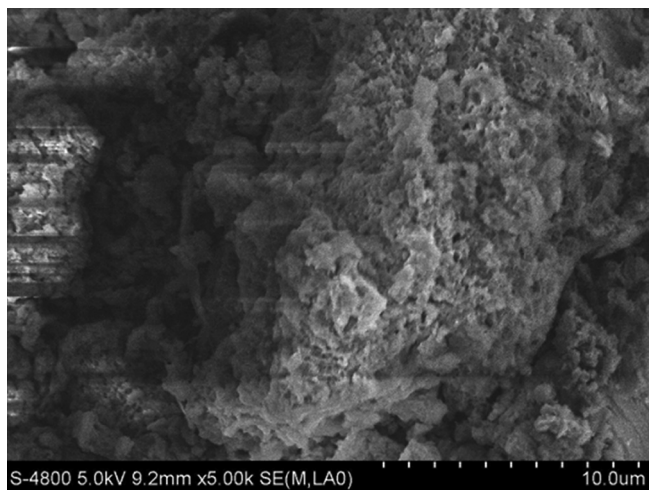


Fig. 3. SEM images of **6d**.

As described in Fig. 4, the configuration of the heterogeneous catalyst **6d** was filiform and loose. And the channels, holes, and cavums were also existed in it. Therefore, substrates would approach the internal catalytic active sites easily in solutions.

3.2. Enantioselective epoxidation of unfunctionalized olefins

The catalytic abilities of immobilized catalyst **6a–d** for the epoxidation of styrene, α -methylstyrene, and indene were studied with *m*-CPBA, NaIO₄, and NaClO as oxidants. Jacobsen's catalyst and

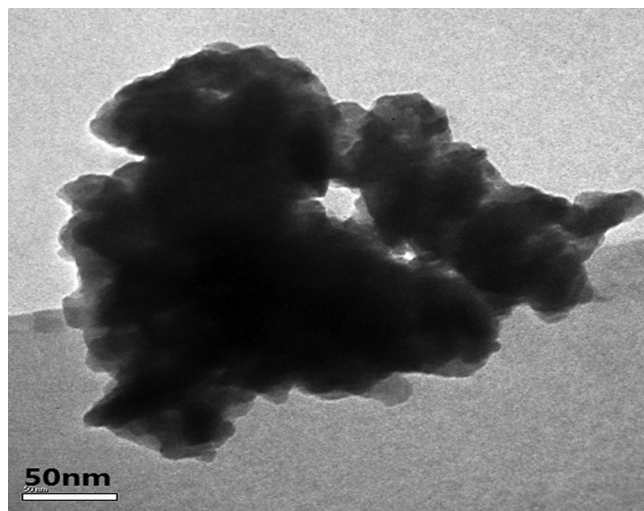


Fig. 4. TEM photograph of the heterogeneous catalyst **6d**.

the homogeneous catalyst **10** were also examined for comparable purposes. The results obtained were summarized in Table 2.

3.2.1. In the oxidative system of *m*-CPBA/NMO. With *m*-CPBA as oxidant, catalyst **6a–d** indicated higher activities than those of Jacobsen's catalyst in the asymmetric epoxidations of α -methylstyrene (ee, 86%–>99% vs 54%, entries 2–5 vs entry 1) and indene (ee, 92.6%–>99% vs 65%, entries 12–15 vs entry 11) as well as styrene (ee, 51.6%–73.46% vs 47%, entries 20–23 vs entry 19). In order to investigate the control of chirality of products, the support ZnPS-PVPA and the 1,2,3-triazole modified ZnPS-PVPA **5d** as well as homogeneous catalyst **10** were applied to epoxidize α -methylstyrene under the same conditions. Obviously, both the support ZnPS-PVPA and the sample **5d** were stereochemically inactive for the epoxidation of olefins (ee, 0% entry 7 and 15.32% entry 8, respectively). Meanwhile, the ee values increased from 54% to 89.6% after chiral salen Mn(III) modified by 1,2,3-triazole (ee, entry 1 vs entry 9) and further increased to >99% (ee, entry 5). On account of these results, it could be deduced that the higher asymmetric induction was owing to the microenvironment of chiral salen Mn(III), the isolation effect of linkage comprising 1,2,3-triazole as well as the special structure of ZnPS-PVPA.

Moreover that ee values increased from 86% to >99%, conversion from 87% to >99% (entries 2–5) with the increase of carbon number of alkylamine in the asymmetric epoxidation of α -methylstyrene, which had been reported by C. Li.²³ The similar varying tendency happened to styrene and indene. For indene, conversions increased from 93.6% to >99%; ee values from 92.6% to >99% (entries 12–15); according to styrene, ee values from 51.6% to 73.46% (entries 20–23). The phenomenon might be owing to the increasing of the linkage making for the immobilized salen Mn(III) complexes approaching the active intermediates of salen Mn(V) or their transition states more easily.

In addition, without the addition of NMO, ee values increased from 13.42% to >99% in the epoxidation of α -methylstyrene (entry 6 vs entry 5). In this context, the supported catalysts did not contain the rigid linker, which could contribute to this phenomenon²⁴ and the bond of Mn–N in the structure of the catalysts had nothing to do with this phenomenon, which was discussed before.²¹ Thus, the special phenomenon could be ascribed to 1,2,3-triazole group in the structure of the catalyst. As it was known, the structure of 1,2,3-triazole group, which was five-membered heterocycle containing three N atoms with lone-pair electron was similar to that of the additive NMO, which possessed six-membered heterocycle

Table 2

Asymmetric epoxidation of styrene, α -methylstyrene, and indene catalyzed by homogeneous **10** and heterogeneous catalysts (**6a–d**) with *m*-CPBA/NMO,^a NaIO₄/imidazole,^b and NaClO/PPNO^c as oxidative systems

Entry	Substrate ^d	Catalyst	Oxidant system	Time (h)	<i>T</i> (°C)	Conv %	ee ^e	TOF ^f × 10 ⁻⁴ (s ⁻¹)
1	A	Jacobsen's	<i>m</i> -CPBA/NMO	5	-40	>99	54	11.11
2	A	6a	<i>m</i> -CPBA	5	-40	87	86	9.76
3	A	6b	<i>m</i> -CPBA	5	-40	89	90	9.99
4	A	6c	<i>m</i> -CPBA	5	-40	92	94	10.32
5	A	6d	<i>m</i> -CPBA	5	-40	>99	>99	11.11
6	A	6d	<i>m</i> -CPBA/NMO	5	-40	>99	13.42	11.11
7	A	1	<i>m</i> -CPBA	5	-40	>99	0	11.11
8	A	5d	<i>m</i> -CPBA	5	-40	>99	15.32	11.11
9	A	10	<i>m</i> -CPBA	5	-40	72	89.6	8.08
10	A	10	<i>m</i> -CPBA/NMO	5	-40	83	82.6	9.31
11	B	Jacobsen's	<i>m</i> -CPBA/NMO	1	0	92	65	51.11
12	B	6a	<i>m</i> -CPBA	1	0	93.6	92.6	52.52
13	B	6b	<i>m</i> -CPBA	1	0	94.2	93.4	52.33
14	B	6c	<i>m</i> -CPBA	1	0	96.4	95.6	53.55
15	B	6d	<i>m</i> -CPBA	1	0	>99	>99	55.55
16	B	6d	<i>m</i> -CPBA/NMO	1	0	35.95	15.62	19.97
17	B	10	<i>m</i> -CPBA	1	0	82.6	90.1	43.66
18	B	10	<i>m</i> -CPBA/NMO	1	0	78.9	87.6	48.3
19	C	Jacobsen's	<i>m</i> -CPBA/NMO	1	0	98	47	54.44
20	C	6a	<i>m</i> -CPBA	1	0	80.6	51.6	44.77
21	C	6b	<i>m</i> -CPBA	1	0	85.2	58.9	47.33
22	C	6c	<i>m</i> -CPBA	1	0	91.6	65.4	50.88
23	C	6d	<i>m</i> -CPBA	1	0	>99	73.46	55.55
24	C	6d	<i>m</i> -CPBA/NMO	1	0	>99	0.93	55.55
25	C	10	<i>m</i> -CPBA	1	0	76.5	57.2	42.50
26	C	10	<i>m</i> -CPBA/NMO	1	0	72.8	54.6	40.44
27	A	Jacobsen's	NaIO ₄ /imidazole	2	25	>99	69	27.78
28	A	6a	NaIO ₄	2	25	>99	>99	27.78
29	A	6b	NaIO ₄	2	25	>99	>99	27.78
30	A	6c	NaIO ₄	2	25	>99	>99	27.78
31	A	6d	NaIO ₄	2	25	>99	>99	27.78
32	A	6d	NaIO ₄ /imidazole	2	25	>99	>99	27.78
33	A	10	NaIO ₄	2	25	82	79	22.78
34	A	10	NaIO ₄ /imidazole	2	25	86	81	23.89
35	A	Jacobsen's	NaClO/PPNO	24	25	>99	65	2.31
36	A	6a	NaClO/PPNO	24	25	85	87	1.96
37	A	6b	NaClO/PPNO	24	25	88	91	2.03
38	A	6c	NaClO/PPNO	24	25	95	96	2.19
39	A	6d	NaClO/PPNO	24	25	>99	>99	2.31
40	A	6d	NaClO	24	25	>99	78.47	2.31
41	A	10	NaClO	24	25	83	68.7	1.91
42	A	10	NaClO/PPNO	24	25	84.5	91.6	1.95

^a Reactions were carried out in CH₂Cl₂ (4 mL) with alkene (1 mmol), *n*-nonane (internal standard, 1 mmol), NMO (5 mmol), homogeneous (5 mol %) or heterogeneous salen Mn(III) catalysts (5 mol %), and *m*-CPBA (2 mmol). The conversion and the ee value were determined by GC with chiral capillary columns HP19091G-B213, 30 m × 0.32 mm × 0.25 μm.

^b Reactions conditions: alkene (1 mmol), NaIO₄ (2 mmol), catalyst (0.03 mmol), CH₃CN/H₂O (10 mL/5 mL).

^c Reactions were carried out in CH₂Cl₂ (2 mL) with PPNO (0.38 mmol) and NaClO (pH 11.5, 0.55 M, 2 mL). Other conditions are the same as aforementioned.

^d A = α -methylstyrene, B = indene, C = styrene.

^e (S)-form.

^f Turnover frequency (TOF) is calculated by the expression of [product]/[catalyst] × time (s⁻¹).

including N and O atom with lone-pair electron. Manifestly, NMO indicated similar electronic effect and spatial effect to 1,2,3-triazole group. Therefore, 1,2,3-triazole group in the supported catalyst not only acted as the linkage and separation group, but also played the role of additive. With the addition of NMO, the steric hindrance from the section of 1,2,3-triazole group in the catalyst made the optimal geometric configuration of the reactive intermediates salen Mn(V)=O or their transition states altered. And then it could lead to olefins approaching salen Mn(V)=O difficultly and the remarkable lower ee values.

3.2.2. In the oxidative system of NaIO₄/imidazole. In the epoxidation of α -methylstyrene with NaIO₄ as oxidant, the heterogeneous catalysts **6a–d** displayed higher catalytic activities than those of Jacobsen's catalyst (ee%, >99 vs 69; entries 28–31 vs entry 27) and comparable catalytic abilities to those of homogeneous catalyst **10**

(conv%, >99 vs 82; ee%, >99 vs 79; entries 28–31 vs 33). Noticeably, through the modification of 1,2,3-triazole chiral salen Mn(III) catalyst **10** indicated 81% ee value, compared with Jacobsen's catalyst (ee, 69%); the ee values kept on increasing from 81% to >99% after the homogeneous catalyst **10** anchored onto ZnPS-PVPA. Based on this, it could demonstrate that the superior catalytic ability was ascribed to cooperativity of ZnPS-PVPA, the linker, and the chiral ligand.

Interestingly, the catalytic abilities that both the conversions and enantioselectivities of the catalysts **6a–d** all exceeded 99% did not increase, but almost were kept unchanged with the increasing of the linkage in NaIO₄/imidazole. It could be due to the oxidative activity of NaIO₄, which was so superior that the length of the linker contributing to the catalytic ability could be neglected.

Apart from this, the superior catalytic activities could still be maintained whether the axial ligand imidazole was added or not.

The additive imidazole scarcely influenced the catalytic activities, which was different to the most results reported. In this context, the structure of imidazole, which was five-membered heterocycle comprising two N atoms with lone-pair electron was similar to that of 1,2,3-triazole group. Apparently, imidazole displayed similar electronic effect to 1,2,3-group and smaller steric configuration according to NMO. Moreover, the spatial hindrance originated in the oxidant NaIO_4 and the axial ligand imidazole could almost be neglected by virtue of the smaller steric configuration. Therefore, 1,2,3-triazole group in the heterogeneous catalyst could be still served as the axial ligand apart from the role of the linkage and isolation group. It was normal whether the axial ligand imidazole was added or not could scarcely contribute to the catalytic activity.

3.2.3. In the oxidative system of NaClO/PPNO . On account of the oxidative system of NaClO/PPNO , the supported catalysts **6a–d** showed higher catalytic abilities than those of Jacobsen's catalyst (conv%, 85→99 vs >99; ee%, 87→99 vs 65; entries 36–39 vs entry 35) and homogeneous catalyst **10** (conv%, 85→99 vs 84.5; ee %, 87→99 vs 91.6; entries 36–39 vs entry 42). By means of chiral salen Mn(III) modified by 1,2,3-triazole, homogeneous catalyst **10** indicated 91.6% ee, according to Jacobsen's catalyst (ee, 65%); the catalytic ability kept on increasing, accompanying with >99% ee value after the catalyst **10** immobilized onto ZnPS-PVPA. The phenomenon also illustrated that the sections of ZnPS-PVPA, linker, and chiral ligand put effects on the catalytic activity.

Simultaneously, the same varied tendency was founded that ee values increased from 87% to >99% and conversions increased from 85% to >99% (entries 28–31) with the increasing of the linkage in the asymmetric epoxidation of α -methylstyrene. The phenomenon had been reported by Li's group²³ and our group,²¹ which was ascribed to the increasing of the linker profiting the catalyst assaulting the reactive intermediate salen Mn(V)=O or transition states.

Apart from this, the additive PPNO played crucial role in the asymmetric epoxidation: ee values increased from 78.47% to >99% with the addition of PPNO, which was at equal to the articles reported.²⁵ In this context, PPNO also could elevate the conversion and enantioselectivity. Although PPNO possessed N and O atoms with lone-pair electron, the steric configuration of PPNO, which was composed of benzene ring connected to pyridine ring was completely differentiated to that of NMO and imidazole. Owing to the bulkier space, the spatial direction of PPNO was certainly stronger than those of NMO and imidazole. That was to say, the semblance of the spatial effect and the electronic effect of 1,2,3-triazole in the supported catalyst was fairly lower to that of PPNO, leading to the role of PPNO not replaced by 1,2,3-triazole. Thereby, it was still necessary for the addition of PPNO that the superior catalytic activity would be obtained in the asymmetric epoxidation with NaClO as oxidant.

3.3. The reusability of the catalyst

The reusability of a heterogeneous catalyst was of great importance from synthetic and economical points of view. To assess the long-term stability and reusability of the supported chiral salen Mn(III) catalysts, α -methylstyrene was used as a model substrate, and recycling experiments were carried out with the catalyst **6d**. The filtrates were collected for determination of Mn leaching.

After recycling for 12 consecutive times, the results were listed in Table 3. Obviously, the catalytic ability decreased slightly after reuse of the catalyst in nine times, accompanying with yield (85.2%) and enantioselectivity (78.93%). The homogeneous catalysts could not recover even one time. In contrast, the supported catalysts **6a–d** could be filtered and reused several times without significant loss of their activity. The effective separating the chiral salen Mn(III)

Table 3

The recycles of catalyst **6d** in the asymmetric epoxidation of α -methylstyrene^a

Run	Time (h)	Conversion (%)	ee (%) ^b	TOF ^c × 10 ⁻⁴ (s ⁻¹)
1	5	>99	>99	11.11
2	5	>99	>99	11.11
3	5	>99	>99	11.11
4	5	>99	98.99	11.11
5	5	96.62	97	10.73
6	5	93.62	95	10.40
7	5	90.67	91.64	10.07
8	5	89.1	86.2	9.90
9	5	85.2	78.93	9.47
10	5	79.31	74.28	8.81
11	5	72.65	23.98	8.07
12	5	32.73	19.97	3.64

^a Reactions were carried out at -40 °C in CH_2Cl_2 (4 mL) with α -methylstyrene (1 mmol), *n*-nonane (internal standard, 1 mmol), *m*-CPBA (0.38 mmol), heterogeneous salen Mn(III) catalysts (5 mol %). The conversion and the ee value were determined by GC with chiral capillary columns HP19091G-B213, 30 m × 0.32 mm × 0.25 μm .

^b Same as in Table 2.

^c Same as in Table 2.

complexes by the solid support ZnPS-PVPA contributed to the good stability of the heterogeneous chiral Mn(III) salen catalyst in case that they would dimerize to inactive μ -oxo-Mn(IV) species. The decrease of the yield could be attributed to the decomposition of the chiral Mn(III) salen complex under epoxidation conditions²⁶ and the loss of the hyperfine granules of the heterogeneous chiral Mn(III) salen catalysts (formed in reaction due to stirring). The Mn content of the heterogeneous catalyst **6d** was 0.48 mmol/g, compared with the total amount (around 0.75 mmol/g) when the heterogeneous catalyst recycled for nine times.

3.4. Large-scale asymmetric epoxidation reaction

We further performed different proportions of large-scale asymmetric epoxidation reactions with α -methylstyrene as substrate and *m*-CPBA as oxidant. The same catalyst loading of 5 mol % as that in the experimental scale was used. The large-scale experiments could be facily carried out using the same procedure as that for the experimental scale reactions. The catalytic results were summarized in Table 4. Delightfully, the conversions and enantioselectivities maintained at the same level for the large-scale reactions under whichever condition that the large scale was 50 times or 100 times (Fig. S3) as much as the experimental scale.

Table 4

Large-scale asymmetric epoxidation reaction of α -methylstyrene^a

Entry	Time (h)	Conversion (%)	ee ^f (%)	TOF ^g × 10 ⁻⁴ (s ⁻¹)
1 ^b	5	>99	>99	11.11
2 ^c	5	>99	>99	11.11
3 ^d	5	>99	98	11.11
4 ^e	5	>99	96	11.11

^a Reactions were carried out at -40 °C in CH_2Cl_2 with α -methylstyrene, *n*-nonane, *m*-CPBA, heterogeneous salen Mn(III) catalysts (5 mol %). The conversion and the ee value were determined by GC with chiral capillary columns HP19091G-B213, 30 m × 0.32 mm × 0.25 μm .

^b The usage amounts of reagents were α -methylstyrene (1 mmol), *n*-nonane (1 mmol), heterogeneous catalyst **3b** (0.05 mmol), *m*-CPBA (2 mmol), respectively.

^c The usage amounts of reagents were α -methylstyrene (50 mmol), *n*-nonane (50 mmol), heterogeneous catalyst **3b** (2.5 mmol), *m*-CPBA (100 mmol), respectively.

^d The usage amounts of reagents were α -methylstyrene (50 mmol), *n*-nonane (50 mmol), heterogeneous catalyst **3b** (0.5 mmol), *m*-CPBA (100 mmol), respectively.

^e The usage amounts of reagents were α -methylstyrene (100 mmol), *n*-nonane (100 mmol), heterogeneous catalyst **3b** (5 mmol), *m*-CPBA (200 mmol), respectively.

^f Same as in Table 2.

^g Same as in Table 2.

4. Conclusions

In summary, the results from the investigation demonstrated that the catalyst **6d** was a robust and effective catalyst for highly enantioselective asymmetric epoxidation reactions. Several types of unfunctionalized olefins could effectively participate in the reaction. Surprisingly, the additive of NMO and imidazole as well as PPNO played different roles in different oxidative systems. The sections of the heterogeneous catalyst, such as the support ZnPS-PVPA, the linker as well as chiral salen Mn center altogether contributed to the superior catalytic ability. The electronic effect and the steric effect of the 1,2,3-triazole group in different oxidative systems as well as the interaction with the additives had been discussed in detail. The catalyst could be readily recovered and reused at least nine times without significant loss of catalytic activity and stereoselectivity. Notably, this metal-catalyzed asymmetric epoxidation could be performed on a large-scale with the enantioselectivity being maintained at the same level, which offered a great possibility for applications in industry.

Acknowledgements

This work was financially supported by National Ministry of Science and Technology Innovation Fund for High-tech Small and Medium Enterprise Technology (NO. 09C26215112399) and National Ministry of Human Resources and Social Security Start-up Support Projects for Students Returned to Business, Office of Human Resources and Social Security Issued 2009 (143) and the Xihua University Key Projects (Z1223321) and Sichuan Province Applied Basic Research Projects (2013JY0090).

Supplementary data

Supplementary data related to this article can be found at <http://dx.doi.org/10.1016/j.tet.2013.04.108>.

References and notes

1. Kolb, H. C.; Finn, M. G.; Sharpless, K. B. *Angew. Chem., Int. Ed.* **2001**, *40*, 2056; *Angew. Chem., Int. Ed.* **2001**, *40*, 2004.
2. *Comprehensive Asymmetric Catalysis I–III*; Jacobsen, E. N., Pfaltz, A., Yamamoto, H., Eds.; Springer: Berlin, 1999.
3. Seayad, J.; List, B. *Org. Biomol. Chem.* **2005**, *3*, 719.
4. Faber, K. *Biotransformations in Organic Synthesis*, 4th ed.; Springer: Berlin, 2000.
5. Thomas, C. M.; Ward, T. R. *Chem. Soc. Rev.* **2005**, *34*, 337.
6. Huisgen, R. *Pure Appl. Chem.* **1989**, *61*, 613.
7. Huisgen, R.; Szeimies, G.; Moebius, L. *Chem. Ber.* **1967**, *100*, 2494.
8. Rostovtsev, V. V.; Green, L. G.; Fokin, V. V.; Sharpless, K. B. *Angew. Chem.* **2002**, *114*, 2708; *Angew. Chem., Int. Ed.* **2002**, *41*, 2596.
9. Bock, V. D.; Hiemstra, H.; van Maarseveen, J. H. *Eur. J. Org. Chem.* **2006**, *1*, 51.
10. Whiting, M.; Muldoon, J.; Lin, Y.-C.; Silverman, S. M.; Lindstrom, W.; Olson, A. J.; Kolb, H. C.; Finn, M. G.; Sharpless, K. B.; Elder, J. H.; Fokin, V. V. *Angew. Chem.* **2006**, *118*, 1463; *Angew. Chem., Int. Ed.* **2006**, *45*, 1435.
11. Lutz, J. F. *Angew. Chem.* **2007**, *119*, 1036; *Angew. Chem., Int. Ed.* **2007**, *46*, 1018.
12. Fournier, D.; Hoogenboom, R.; Schubert, U. S. *Chem. Soc. Rev.* **2007**, *36*, 1369.
13. DVaz, D. D.; Rajgopal, K.; Strable, E.; Schneider, J.; Finn, M. G. *J. Am. Chem. Soc.* **2006**, *128*, 6056.
14. (a) Angell, Y. L.; Burgess, K. *Chem. Soc. Rev.* **2007**, *36*, 1674 Prominent examples include; (b) Horne, W. S.; Yadav, M. K.; Stout, C. D.; Ghadiri, M. R. *J. Am. Chem. Soc.* **2004**, *126*, 15366; (c) Horne, W. S.; Stout, C. D.; Ghadiri, M. R. *J. Am. Chem. Soc.* **2003**, *125*, 9372; (d) Angelo, N. G.; Arora, P. S. *J. Am. Chem. Soc.* **2005**, *127*, 17134.
15. Welbes, L. L.; Scarrow, R. C.; Borovik, A. S. *Chem. Commun.* **2004**, 2544.
16. Ready, J. M.; Jacobsen, E. N. *Angew. Chem., Int. Ed.* **2002**, *41*, 1374.
17. Baleizão, C.; Gigante, B.; Garcia, H.; Corma, A. *Green Chem.* **2002**, *4*, 272.
18. Maria, P. D. *Angew. Chem., Int. Ed.* **2008**, *47*, 2.
19. Zhang, W.; Loebach, J. L.; Wilson, S. R.; Jacobsen, E. N. *J. Am. Chem. Soc.* **1990**, *112*, 2801.
20. Zhang, W.; Lee, N. H.; Jacobsen, E. N. *J. Am. Chem. Soc.* **1994**, *116*, 425.
21. Gong, B. W.; Fu, X. K.; Chen, J. X.; Li, Y. D.; Zou, X. C.; Tu, X. B.; Ding, P. P.; Ma, L. P. *J. Catal.* **2009**, *262*, 9.
22. Huang, J.; Fu, X. K.; Wang, G.; Li, C.; Hu, X. Y. *Dalton Trans.* **2011**, *40*, 3631.
23. Zhang, H. D.; Zhang, Y. M.; Li, C. *J. Catal.* **2006**, *238*, 369.
24. Zou, X. C.; Fu, X. K.; Li, Y. D.; Tu, X. B.; Fu, S. D.; Luo, Y. F.; Wu, X. J. *Adv. Synth. Catal.* **2010**, *352*, 163.
25. Zhang, H. D.; Zhang, Y. M.; Li, C. *Tetrahedron: Asymmetry* **2005**, *16*, 2417.
26. Song, C. E.; Roh, E. J.; Yu, B. M.; Chi, D. Y.; Kim, S. C.; Lee, K. J. *Chem. Commun.* **2000**, 615.